Electronic Supplementary Material

CeO_x-Modified RhNi Nanoparticles Grown on rGO as Highly Efficient Catalysts for Complete Hydrogen Generation from Hydrazine Borane and Hydrazine

Zhujun Zhang, Zhang-Hui Lu,* Hongliang Tan, Xiangshu Chen,* Qilu Yao

Jiangxi Inorganic Membrane Materials Engineering Research Centre, College of Chemistry and Chemical Engineering, Jiangxi Normal University, Nanchang 330022, China.

*E-mails: luzh@jxnu.edu.cn (Z.-H. Lu).

Synthesis of hydrazine borane

Typically, 80 mL of anhydrous dioxane containing 21.42 g of hydrazine hemisulfate salt ($N_2H_4 \cdot 1/2H_2SO_4$) and 10 g of sodium borohydride ($NaBH_4$) were stirred at 30 ^oC under an atmosphere of dry argon for 48 h. The resulting slurry was immediately subjected to 12 min of centrifugation at 12000 r.p.m to get the clear solution. Then, the filtrate was evaporated by vacuum dryer at 40 ^oC over night to get the raw $N_2H_4BH_3$, which was further washed with n-pentene. The resulting product is a white solid with a purity of >99% verified by ^1H and ^{11}B solution-state NMR by using a Bruker 400M liquid ^{1}HNMR using CD_3CN as solvent (Fig. S26). ^1H NMR (δ/ppm, 400 MHz, CD_3CN, 295.4 K, J/Hz): δ 5.45 (s, 1H), 3.51 (d, J = 69.9 Hz, 1H), 1.85 – 0.88 (m, 2H). ^{11}B NMR (δ/ppm, 128 MHz, CD_3CN, 295.3 K, J/Hz): δ -17.37 (s), -18.12 (s), -19.23 (d, J = 95.5 Hz), -20.48 – -77.28 (m).

The redox reaction between $Ce(OH)_3$ and Rh^{3+} or O_2.

$3Ce(OH)_3 + Rh^{3+} \rightarrow Rh + 3CeO_2 + 3H_2O + 3H^+$ eqn. (S1)

$4Ce(OH)_3 + O_2 \rightarrow 4CeO_2 + 6H_2O$ eqn. (S2)

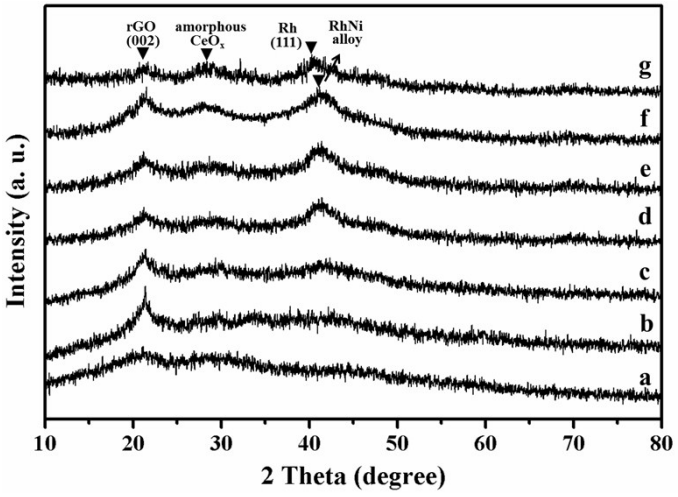

Fig. S1 Powder XRD patterns of the obtained (a) Ni@CeO_x/rGO, (b) $Rh_{0.1}Ni_{0.9}$@CeO_x/rGO, (c) $Rh_{0.3}Ni_{0.7}$@CeO_x/rGO, (d) $Rh_{0.5}Ni_{0.5}$@CeO_x/rGO, (e) $Rh_{0.7}Ni_{0.3}$@CeO_x/rGO, (f) $Rh_{0.8}Ni_{0.2}$@CeO_x/rGO and (g) Rh@CeO_x/rGO catalysts.

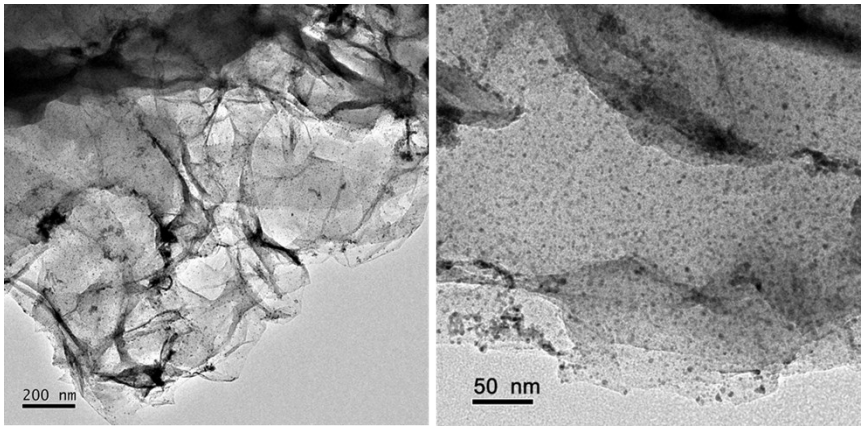

Fig. S2 TEM images of $Rh_{0.8}Ni_{0.2}$@CeO_x/rGO NCs with different magnifications.

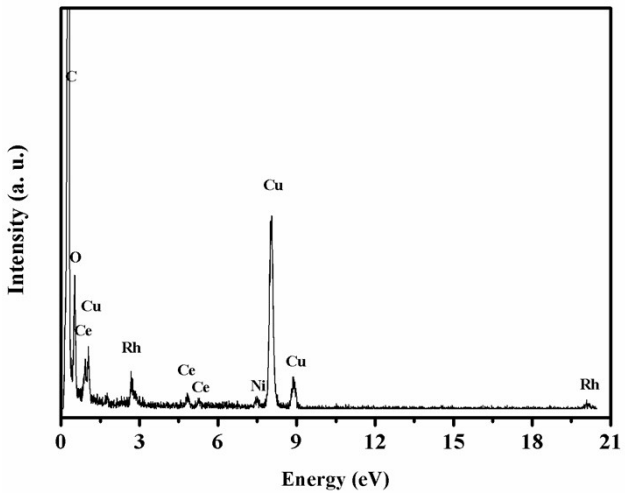

Fig. S3 EDX pattern of $Rh_{0.8}Ni_{0.2}$@CeOx/rGO NCs.

Table S1. Catalysts composition determined by inductively coupled plasma atomic emission spectroscopic (ICP-AES).

Catalysts	Rh (wt%)	Ni (wt%)	Ce (wt%)	Rh:Ni:Ce (atomic ratio)
$Rh@CeO_2/rGO$	42.1	~	9.8	41:0: 7
Ni@CeOx/rGO		31.6	12.0	0: 54: 9
$Rh_{0.8}Ni_{0.2}@CeO_x/rGO$	35.1	5.3	10.2	34: 9:7
$Rh_{0.8}Ni_{0.2}$ /rGO	40.2	6.5	~	39:11:0
$Rh_{0.8}Ni_{0.2}@CeO_x$	~	~	~	73:17:14

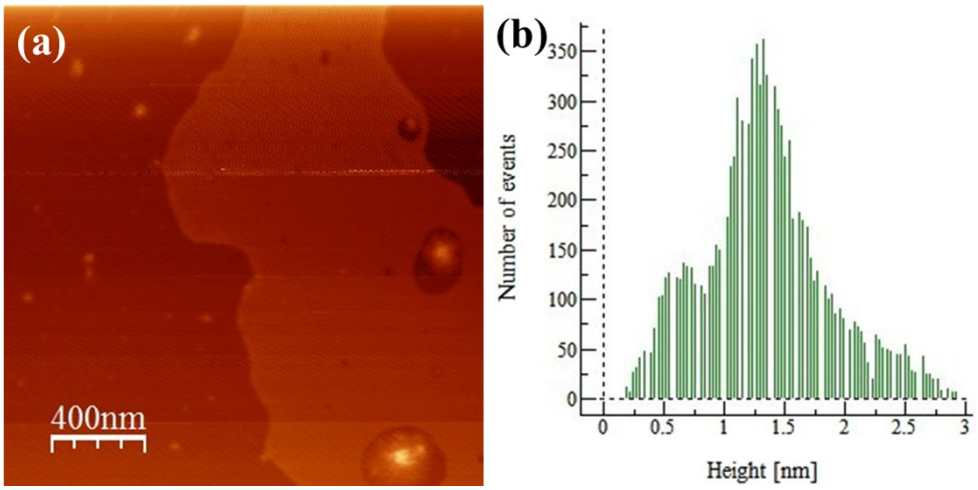

Fig. S4 (a) AFM image and (b) normal distribution of the height of GO.

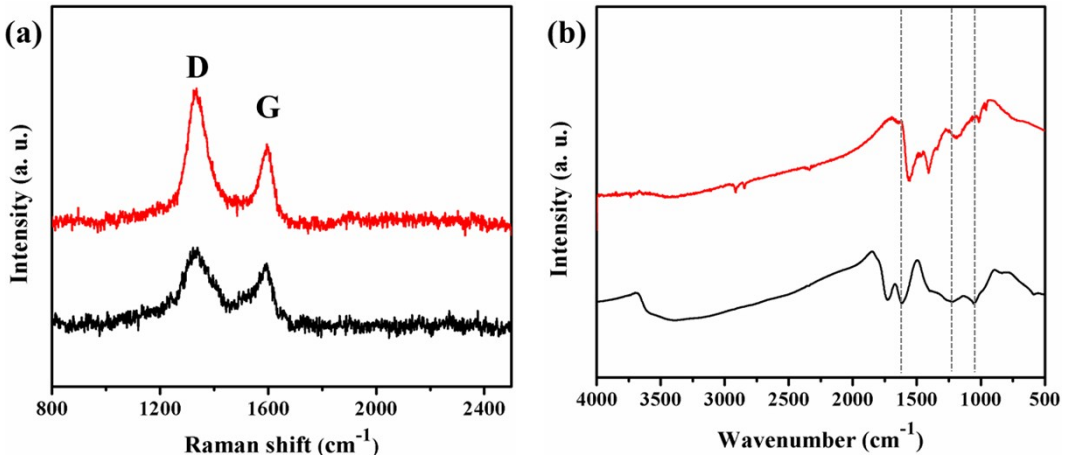

Fig. S5 (a) Raman and (b) FTIR spectra of GO and $Rh_{0.8}Ni_{0.2}@CeO_x$/rGO NCs.

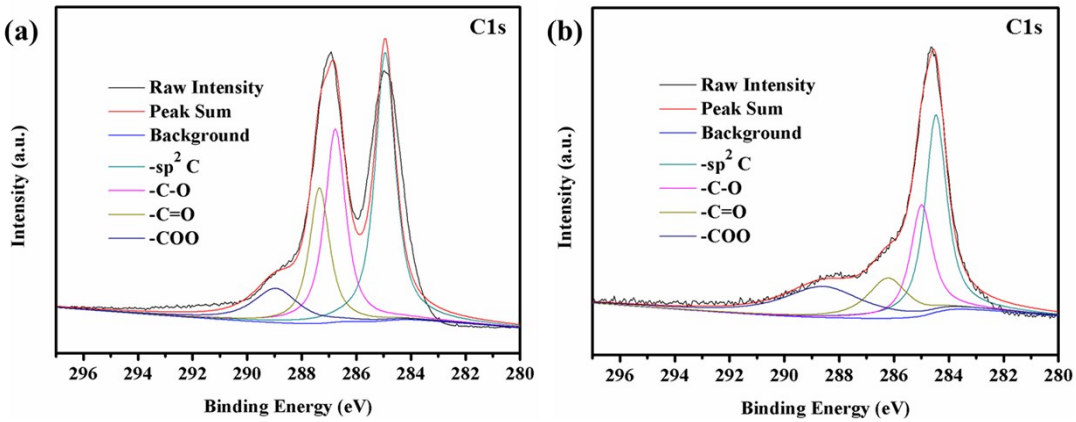

Fig. S6 XPS spectrum of C 1s for (a) GO and (b) $Rh_{0.8}Ni_{0.2}@CeO_x$/rGO NCs.

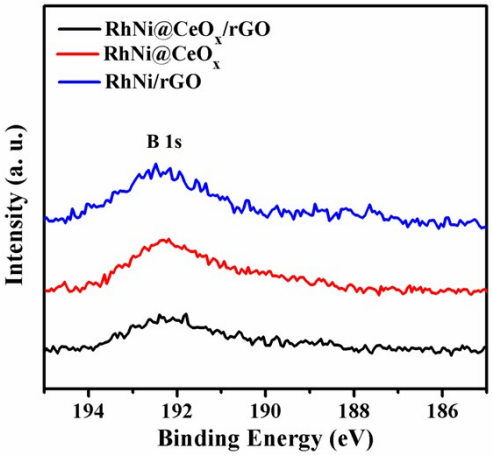

Fig. S7 XPS spectra of B 1s for the synthesized catalysts.

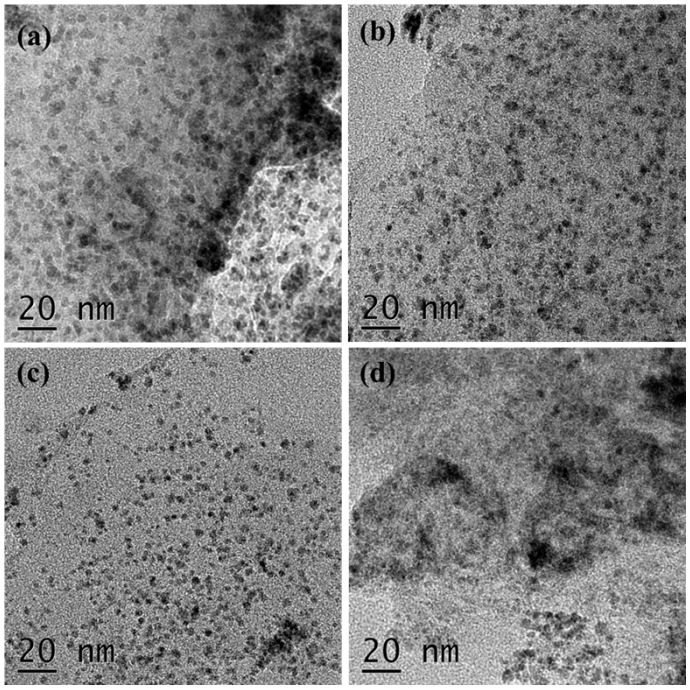

Fig. S8 TEM images of $Rh_{0.8}Ni_{0.2}$@CeO_x/rGO NCs prepared with (a) 0; (b) 7.5; (c) 15; and (d) 35 mg of CTAB.

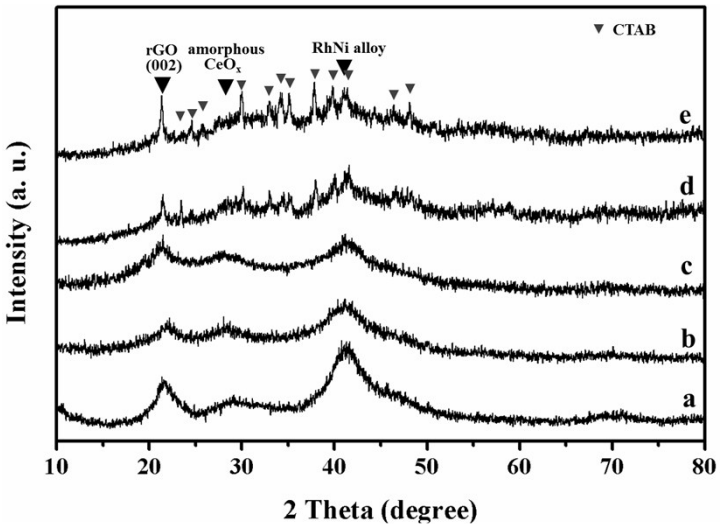

Fig. S9 XRD patterns of $Rh_{0.8}Ni_{0.2}$@CeO_x/rGO NCs prepared with (a) 0; (b) 7.5; (c) 15; (d) 25 and (e) 35 mg of CTAB.

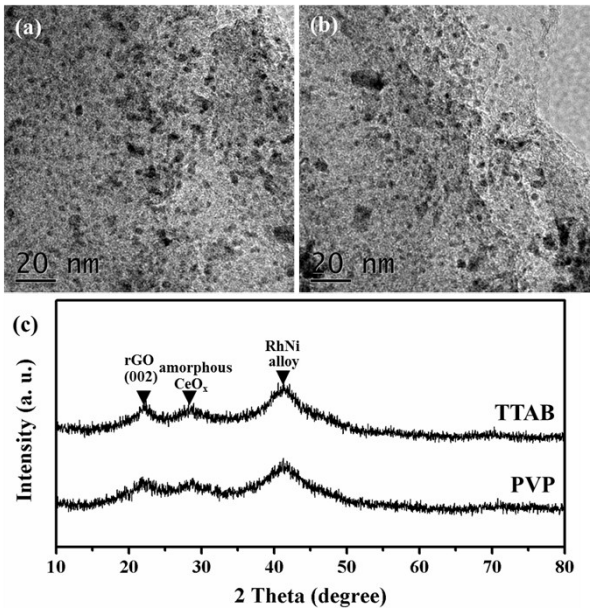

Fig. S10 TEM images of $Rh_{0.8}Ni_{0.2}@CeO_x$/rGO NCs prepared with (a) PVP and (b) TTAB; (c) XRD patterns of $Rh_{0.8}Ni_{0.2}@CeO_x$/rGO NCs prepared with PVP and TTAB.

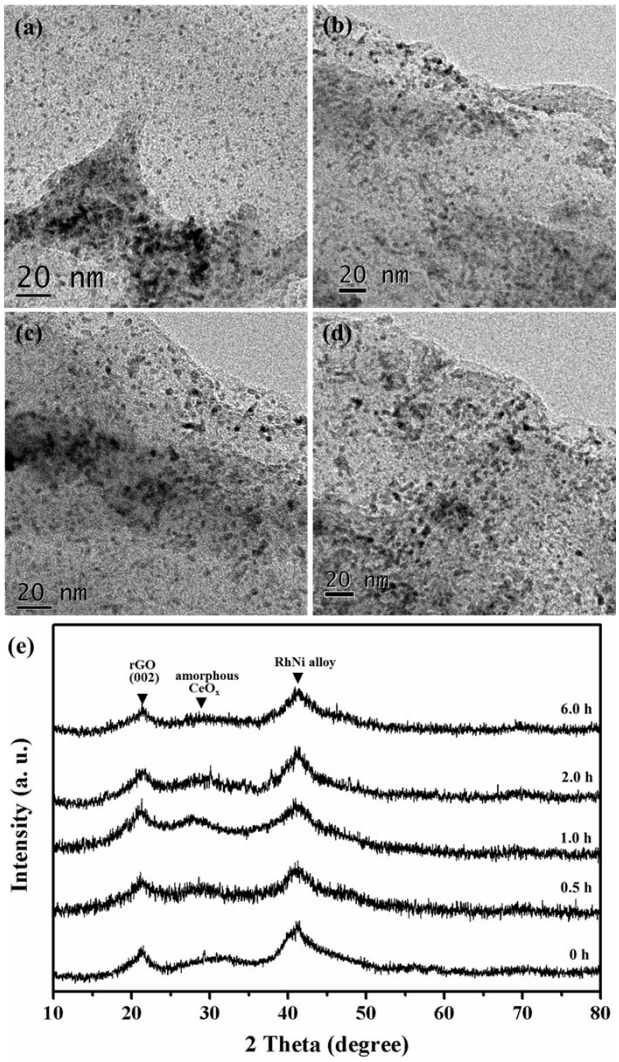

Fig. S11 TEM images of $Rh_{0.8}Ni_{0.2}$@CeO_x/rGO NCs prepared by stirring (a) 0 h; (b) 0.5 h; (c) 2.0 h; and (d) 6.0 h during the impregnation period. (e) XRD patterns of $Rh_{0.8}Ni_{0.2}$@CeO_x/rGO NCs prepared with different stirring time during the impregnation period.

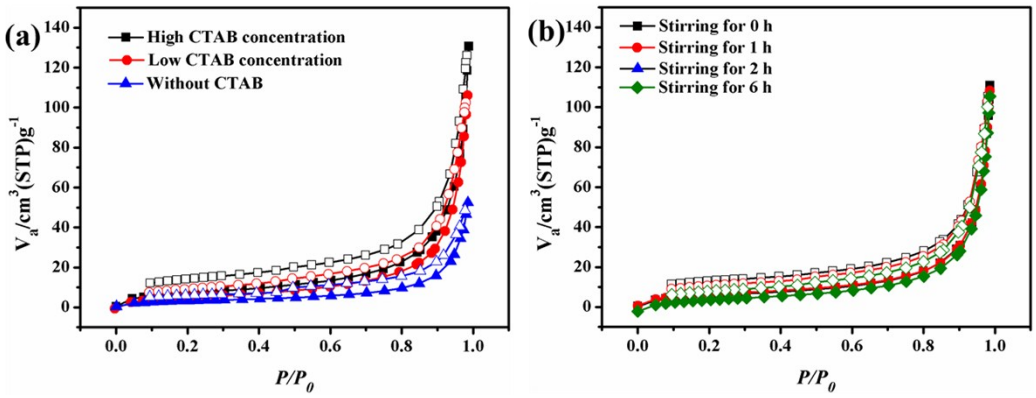

Fig. S12 Nitrogen adsorption-desorption isotherms of RhNi@CeO_x/rGO prepared in (a) different CTAB concentrations (High: 35 mg; Low: 15 mg) and (b) by different stirring times during the impregnation period after dehydration under vacuum at 100 °C for 8 h using BELSORP-mini II.

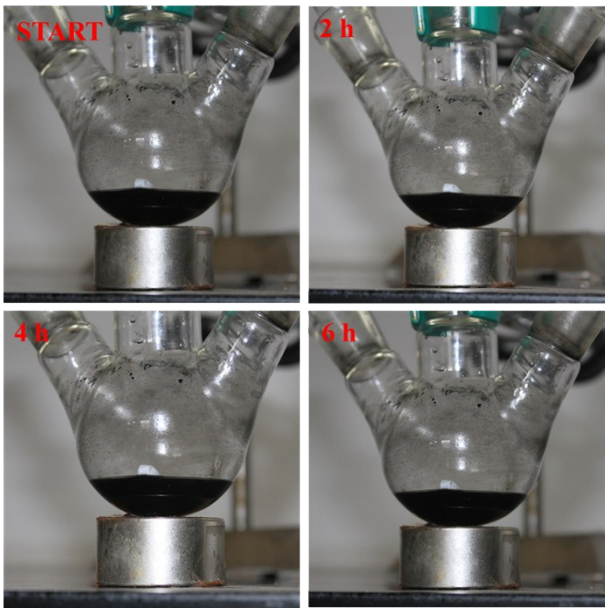

Fig. S13 Pictures of the as prepared RhNi@CeO_x/rGO suspensions contact with a ferromagnetic magnet for a period of time.

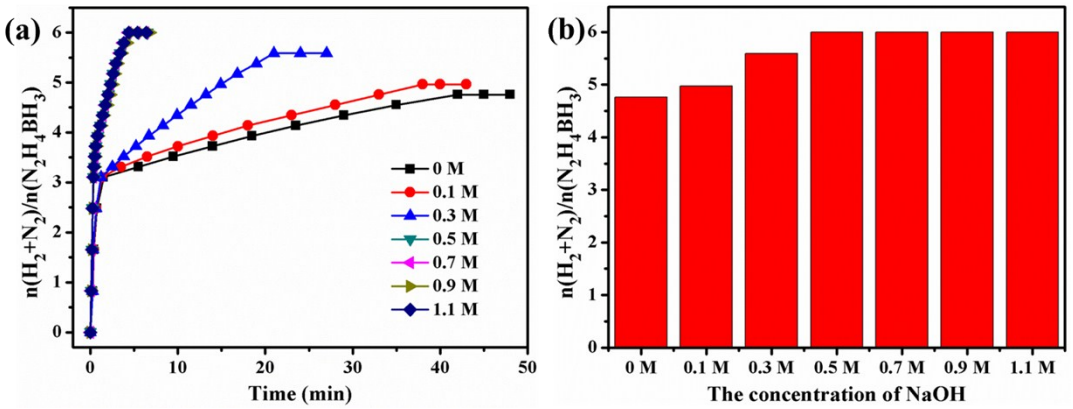

Fig. S14 (A) Time course plots for H_2 generation from $N_2H_4BH_3$ (200 mM, 5 mL) over $Rh_{0.8}Ni_{0.2}@CeO_x/rGO$ (13.9 mol% Ce; $n_{(Ni+Rh)}/n_{(N2H4BH3)}$ = 0.1) with different molar concentration of NaOH at 323 K. (B) The corresponding yield of H_2 and N_2 per mole $N_2H_4BH_3$.

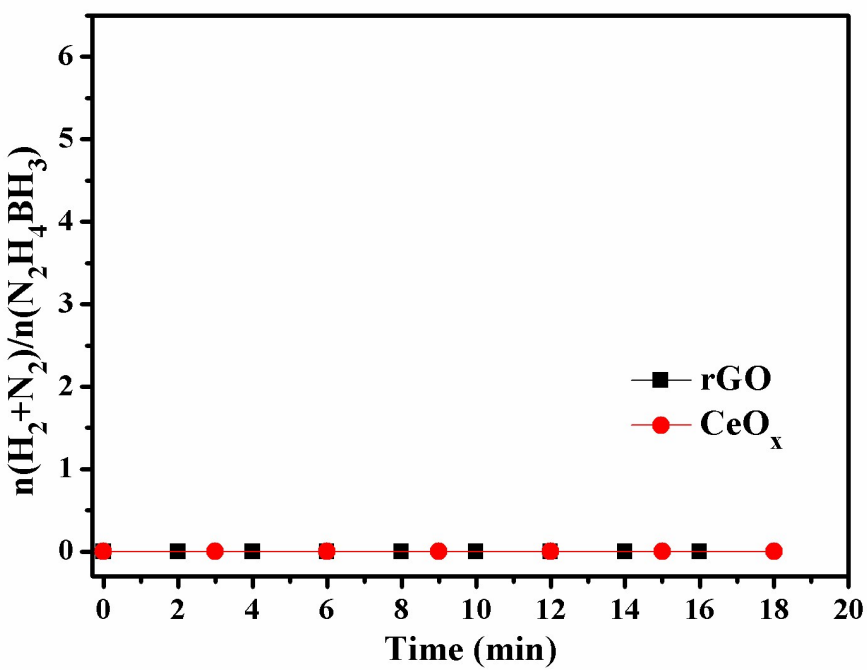

Fig. S15 Time course plots for hydrogen generation from $N_2H_4BH_3$ (200 mM, 5 mL) over rGO or CeO_x with NaOH (0.5 M) at 323 K.

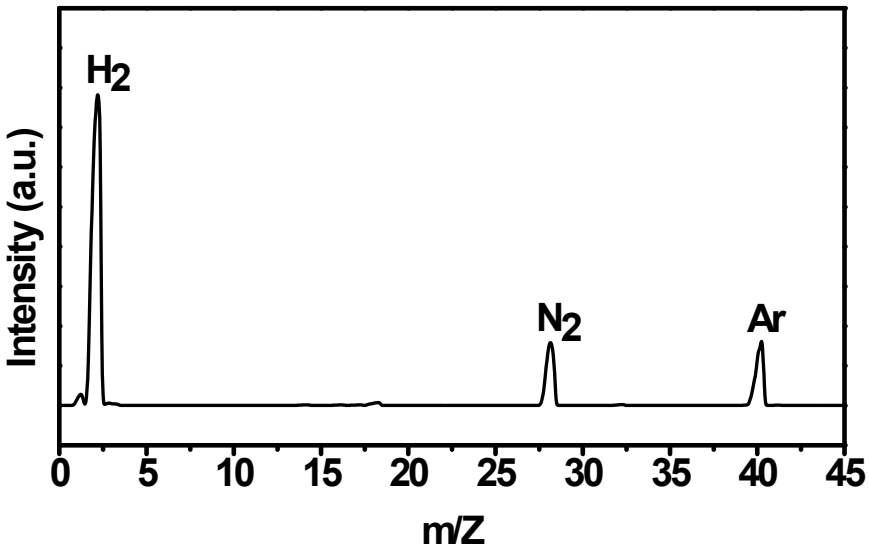

Fig. S16 Mass spectral profile for gases released from $N_2H_4BH_3$ using $Rh_{0.8}Ni_{0.2}$@CeO_x/rGO NCs under an argon atmosphere.

Table S2. Comparison of activity of different catalysts for hydrogen generation from $N_2H_4BH_3$ at 323K.

Entry	Catalysts	$n(H_2+N_2)/n(HB)$	TOF (h^{-1})	Ref.
1	Ni_5@Pt	4.4	2.3[a]	11
2	$Ni_{0.89}Ir_{0.11}$ NPs	4.9	9.5[a]	12
3	$Ni_{0.89}Rh_{0.11}$ NPs	5.1	9.9[a]	12
4	$Ni_{0.77}Ru_{0.23}$ NPs	4.0	23.3[a]	12
5	$Ni_{0.89}Pt_{0.11}$ NPs	5.79	18.0[a]	10
6	Ni@(Rh_4Ni-alloy)/Al_2O_3	5.74	72.0[a]	14
7	Rh_4Ni NPs	5.8	90[b]	37
8	$Ni_{0.9}Pt_{0.1}$-CeO_2	5.74	234[b]	47
9	$Ni_{0.9}Pt_{0.1}$/graphene	6.0	240[b]	50
10	$Rh_{0.8}Ni_{0.2}$-CeO_x	5.83	228.5	This work
11	$Rh_{0.8}Ni_{0.2}$/rGO	6.0	206.9	This work
12	$Rh_{0.8}Ni_{0.2}$@CeO_x/rGO	6.0	666.7	This work

[a]The total TOF values were calculated according to the original data provided by the reports, in which the TOF values were not provided.

[b]The total TOF values were provided by the reports.

Calculation method for TOF

The total turn-over frequency (TOF) reported in this work is an apparent TOF value based on the number of metal (Rh + Ni) atoms in catalysts, which is calculated from the equation as follows:

$$TOF = \frac{n_{H_2}}{n_{(Rh+Ni)} \times t} \qquad (1)$$

Where n_{H2} is the mole number of generated H_2, $n_{(Rh+Ni)}$ is the total mole number of Ni and Rh in catalyst and *t* is the completed reaction time in hour. The TOF values of all the cited catalysts shown in Table S2 are the total TOF values and are normalized to the mass of metals.

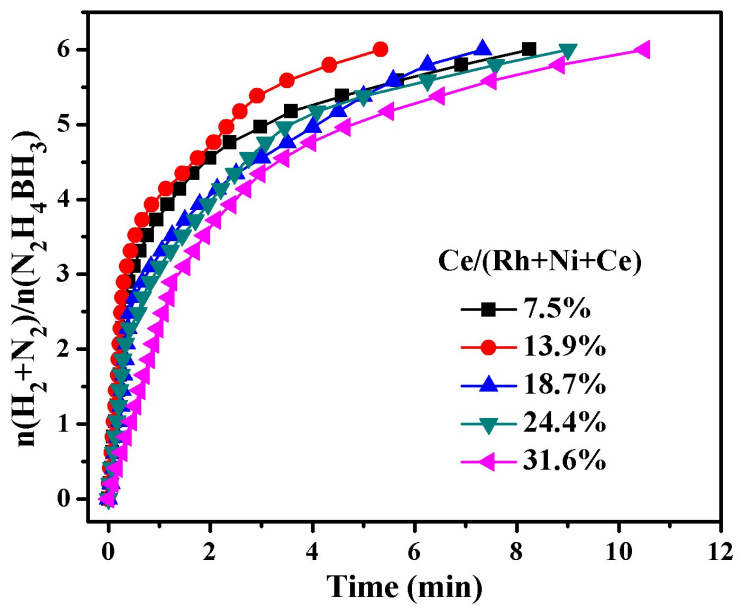

Fig. S17 Time course plots for H_2 generation from $N_2H_4BH_3$ (200 mM, 5 mL) over $Rh_{0.8}Ni_{0.2}@CeO_x$/rGO NCs with different molar content of Ce ($n_{(Ni+Rh)}/n_{(N2H4BH3)}$ = 0.1) in the presence of NaOH (0.5 M) at 323 K.

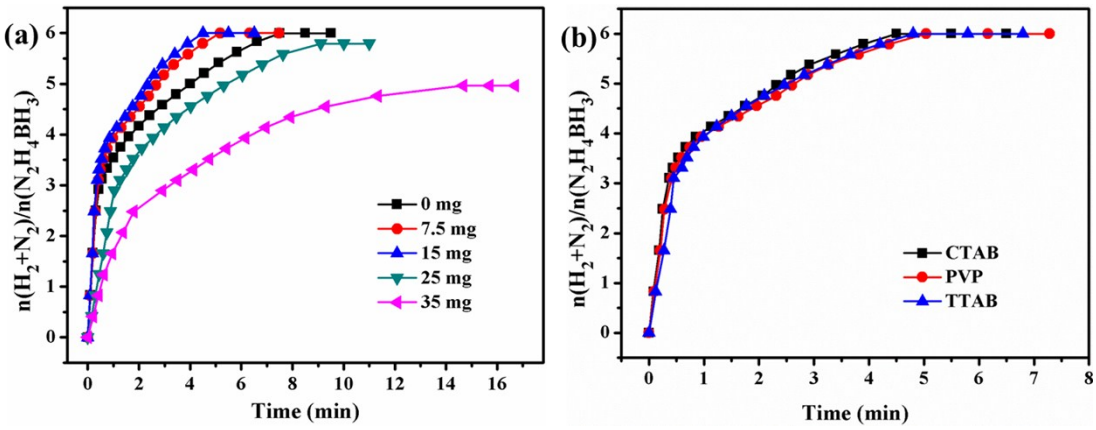

Fig. S18 Time course plots for H_2 generation from $N_2H_4BH_3$ (200 mM, 5 mL) over $Rh_{0.8}Ni_{0.2}$@CeO_x/rGO NCs prepared with (a) different CTAB concentrations and (b) different surfactants ($n_{(Ni+Rh)}/n_{(N2H4BH3)}$ = 0.1) in the presence of NaOH (0.5 M) at 323 K.

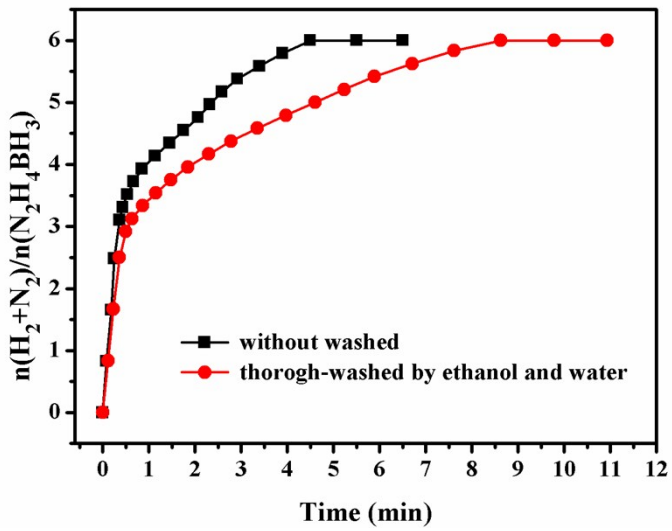

Fig. S19 Time course plots for H_2 generation from $N_2H_4BH_3$ (200 mM, 5 mL) over $Rh_{0.8}Ni_{0.2}$@CeO_x/rGO NCs with thorogh-washed by ethanol and water or without washed ($n_{(Ni+Rh)}/n_{(N2H4BH3)}$ = 0.1) in the presence of NaOH (0.5 M) at 323 K.

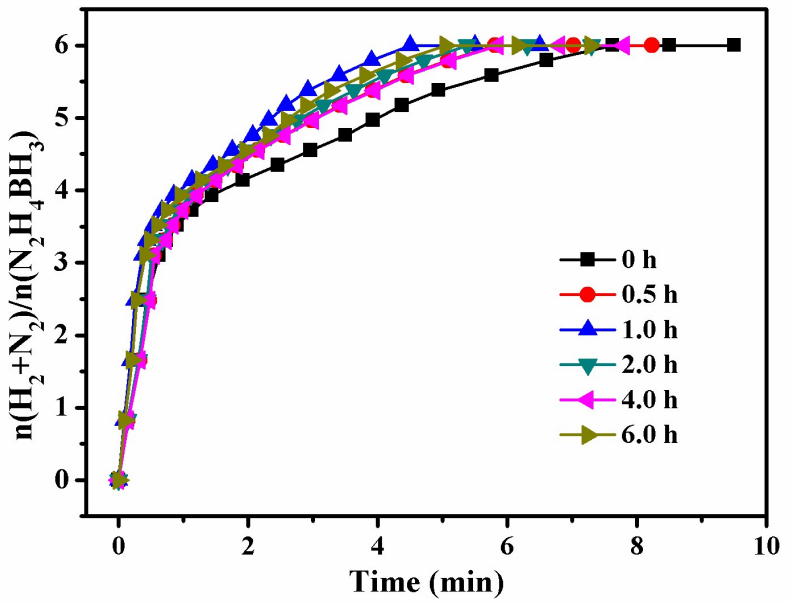

Fig. S20 Time course plots for H_2 generation from $N_2H_4BH_3$ (200 mM, 5 mL) over $Rh_{0.8}Ni_{0.2}$@CeO_x/rGO NCs prepared by stirring with different times during the impregnation period ($n_{(Ni+Rh)}/n_{(N2H4BH3)}$ = 0.1) in the presence of NaOH (0.5 M) at 323 K.

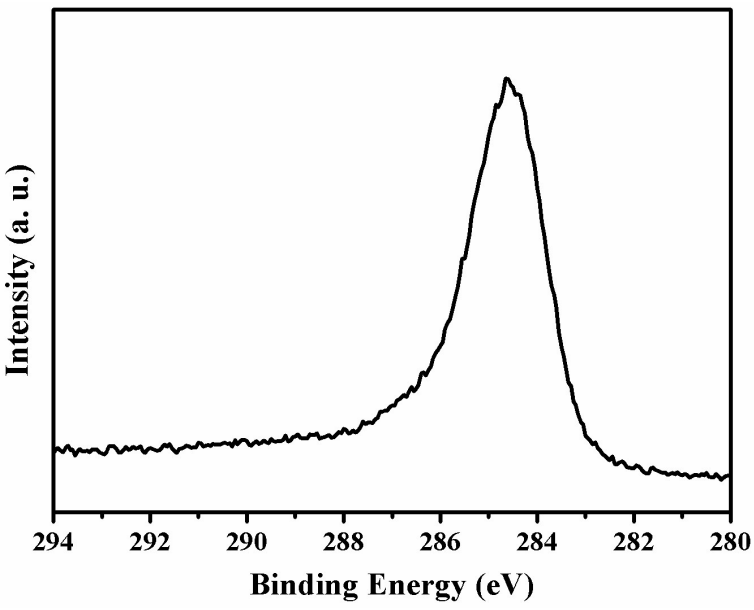

Fig. S21 XPS spectra for C 1s of $Rh_{0.8}Ni_{0.2}@CeO_x$/rGO NCs synthesized by using an excess amount (40 mg) of $NaBH_4$.

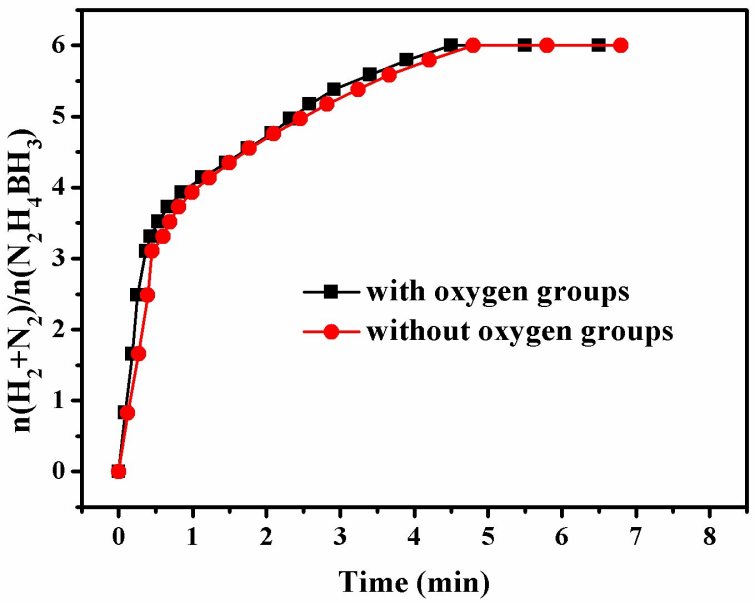

Fig. S22 Time course plots for H_2 generation from $N_2H_4BH_3$ (200 mM, 5 mL) over $Rh_{0.8}Ni_{0.2}$@CeO_x/rGO NCs with or without residual oxygen groups ($n_{(Ni+Rh)}/n_{(N2H4BH3)}$ = 0.1) in the presence of NaOH (0.5 M) at 323 K.

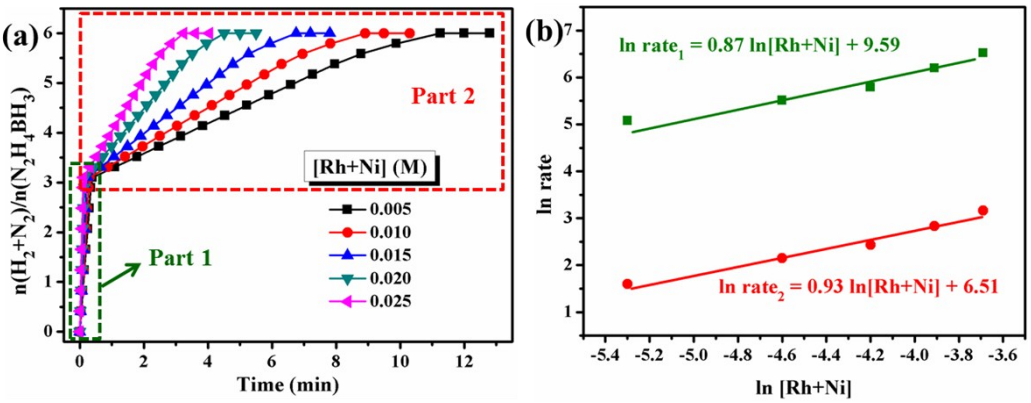

Fig. S23 Time course plots for H_2 generation from $N_2H_4BH_3$ showing (a) hydrolysis of BH_3 group (Part 1) and decomposition of N_2H_4 moiety (Part 2) of $N_2H_4BH_3$ (13.9 mol% Ce; n(Ni+Rh)/n($N_2H_4BH_3$ or N_2H_4) = 0.1) at different [Rh+Ni] concentrations. (b) Plot of ln *rate* versus ln [Rh+Ni] during H_2 generation from hydrolysis of BH_3 group and decomposition of N_2H_4 moiety at different [Rh+Ni] concentrations.

Table S3. Comparison of the catalytic performance of different catalysts for H_2 generation by N_2H_4 decomposition.

Catalyst	T (℃)	$n_{(metal)}/n_{(N_2H_4)}$	H_2 selectivity	Reaction times (min)	E_a (kJ/mol)	TOF (h^{-1})	Ref.
Rh_4Ni	25	0.1	100%	160	-	7.5[a]	36
Rh_4Ni/graphene	25	0.1	100%	49	-	24.5[a]	52
$Ni_{0.9}Pt_{0.1}/Ce_2O_3$	25	0.1	100%	43	42.3	27.9[a] (28.1[b])	33
$Ni_{0.90}Pt_{0.05}Rh_{0.05}/La_2O_3$	25	0.1	100%	18	-	66.7[a] (45.9[b])	29
Ni_3Pt_7/graphene	25	0.005	100%	-	49.36	68[c]	34
Fe-B/MWCNTs	25	-	97%	-	46.7	4032[c]	59
Co-B honeycomb	25	-	41.8%	-	54.3	756[c]	60
Ni-Al_2O_3-HT	30	-	93%	70	-	-	21
$NiPt_{0.057}/Al_2O_3$	30	-	97%	11.5	34.0	16.5[c]	22
Ni-0.080CeO_2	30	-	99%	-	47.0	51.6[c]	46
RhNi-B	30	0.1	100%	22	-	54.5[a]	17
$Pt_{60}Ni_{40}$-CNDs	30	0.1	100%	7.0	43.9	170[a]	18
$Rh_{0.8}Ni_{0.2}@CeO_x$/rGO	30	0.1	100%	33	58.0	36.4	this work
NiMoB/$La(OH)_3$	50	0.3	100%	15	55.1	26.7[a]	32
$Ni_{0.6}Fe_{0.4}Mo$	50	0.2	100%	15	50.7	40[a] (28.8[b])	20
$Ni_{80}Pt_{20}$@ZIF-8	50	0.067	100%	26	-	68.9[a] (90[b])	26
$Ni_{66}Rh_{34}$@ZIF-8	50	0.072	100%	-	58.01	140[c]	27
$Rh_{0.8}Ni_{0.2}@CeO_x$/rGO	50	0.1	100%	5.7	58.0	210.5	this work
$Rh_{0.8}Ni_{0.2}@CeO_x$/rGO	60	0.1	100%	3.0	58.0	400	this work
NiFe	70	0.1	100%	190	-	6.3[a]	24
$Cu@Fe_5Ni_5$	70	0.11	100%	60.0	79.2	18.2[a]	25

[a]The total TOF values were calculated according to the original data provided by the reports.

[b]The initial TOF values were provided by the reports.

[c]The TOF values were provided by the reports, in which the calculation method of TOF and total reaction time (or metal molar content) were not given clearly.

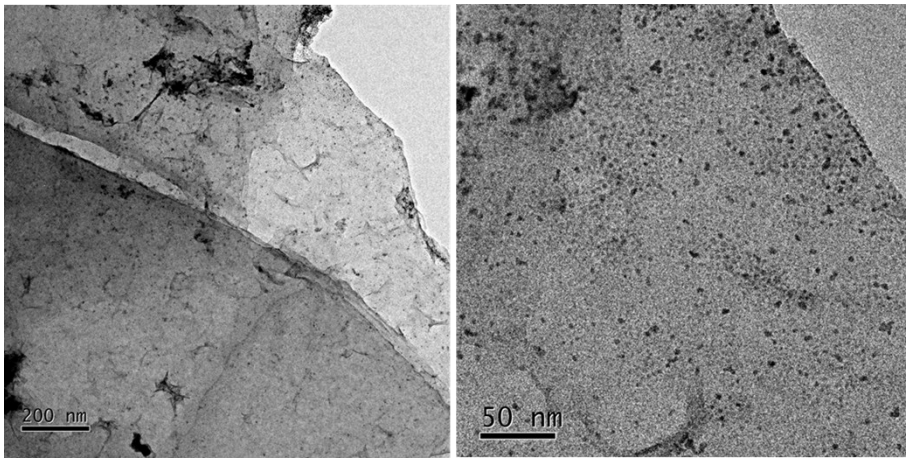

Fig. S24 TEM images of $Rh_{0.8}Ni_{0.2}$@CeO_x/rGO NCs after the durability and reusability test with different magnifications.

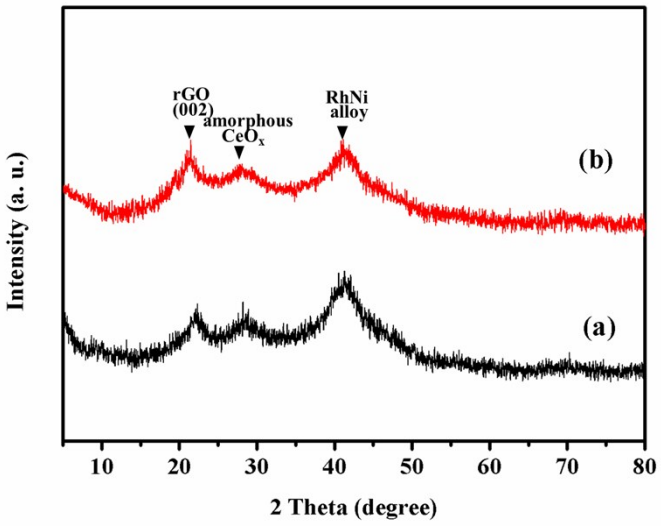

Fig. S25 Powder XRD patterns of (a) fresh synthesized $Rh_{0.8}Ni_{0.2}$@CeO_x/rGO NCs and (b) the $Rh_{0.8}Ni_{0.2}$@CeO_x/rGO NCs after the durability and reusability test.

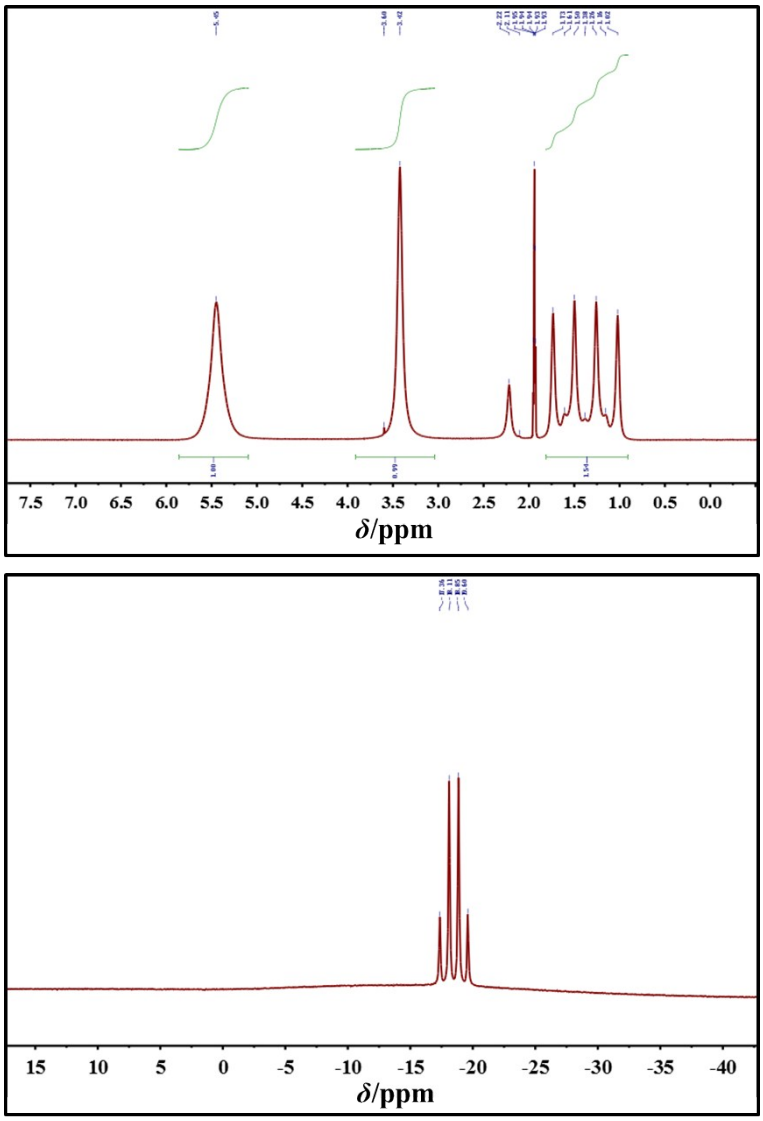

Fig. S26 ^{1}H (top) and ^{11}B (bottom) solution-state NMR spectra of the as-synthesized hydrazine borane in CD_3CN. These spectra show that hydrazine borane is synthesized with a purity of >99%.